Revealing rearrangement of local short-range order in metastable liquid metal under static magnetic field

Rong Fu[1,2,3*], Musen Li[2,4], Tianhao Su[4], Bo Chen[1], Weidong Xuan[1*], He Lin[5], Jianfeng Ji[5], Michael Cortie[2], Danica Solina[2*] & Zhongming Ren[1]

[1]State Key Laboratory of Advanced Special Steel, School of Materials Science and Engineering, Shanghai University, Shanghai 200444, China.

[2]School of Mathematical and Physical Sciences, University of Technology Sydney, New South Wales 2007, Australia.

[3]Australian Nuclear Science and Technology Organization, New Illawarra Road, Lucas Heights, NSW 2232, Australia.

[4]Materials Genome Institute, Shanghai University, Shanghai 200444, China.

[5]Shanghai Synchrotron Radiation Facility, Shanghai Advanced Research Institute, Chinese Academy of Sciences, Shanghai 201204, China.

This PDF file includes:

Fig. S1 to S4

Tables S1.

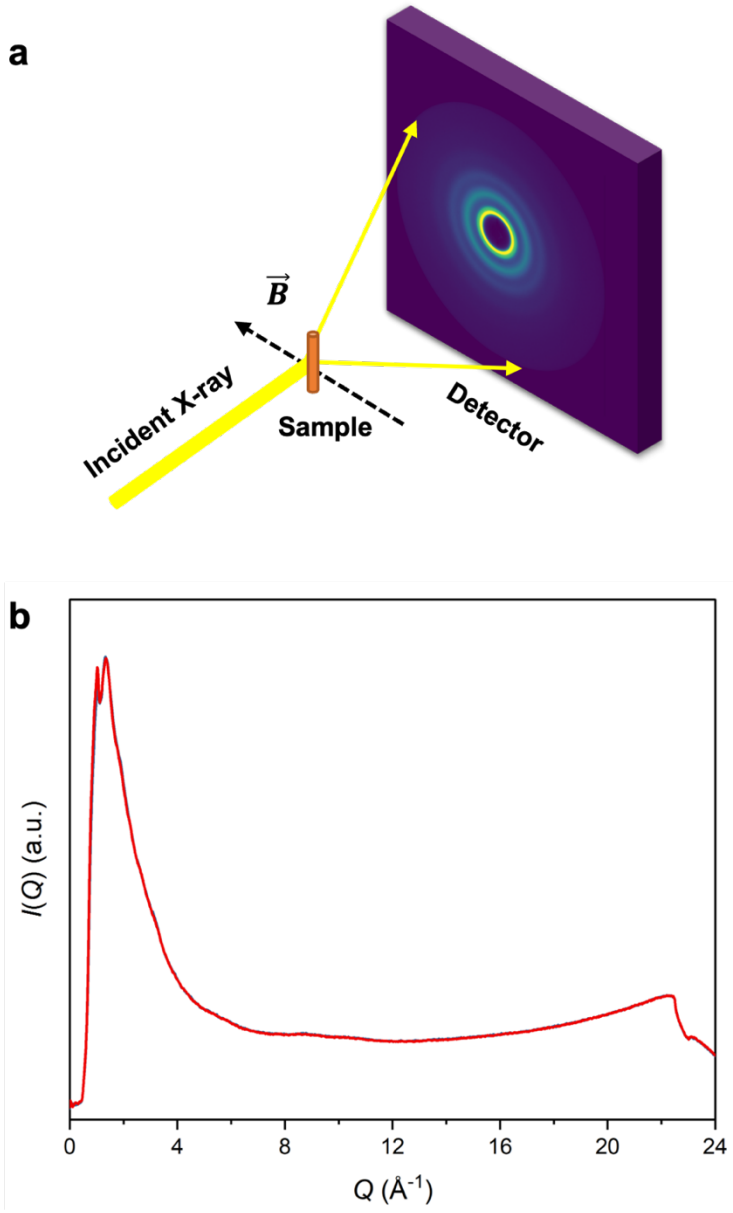

Fig. S1. (a) Schematic of in-situ high-energy synchrotron X-ray total scattering setup, where the field direction ($\vec{B}$) is perpendicular to the sample capillary. The incident X-ray penetrated liquid metal sample capillary, leaving diffuse Debye-Scherrer rings on the area detector. **(b)** Scattering functions, $I(Q)$ of empty capillary under 0 T (blue curve) and 0.2 T SMF (red curve), and intensity has been normalized by the total photon energy.

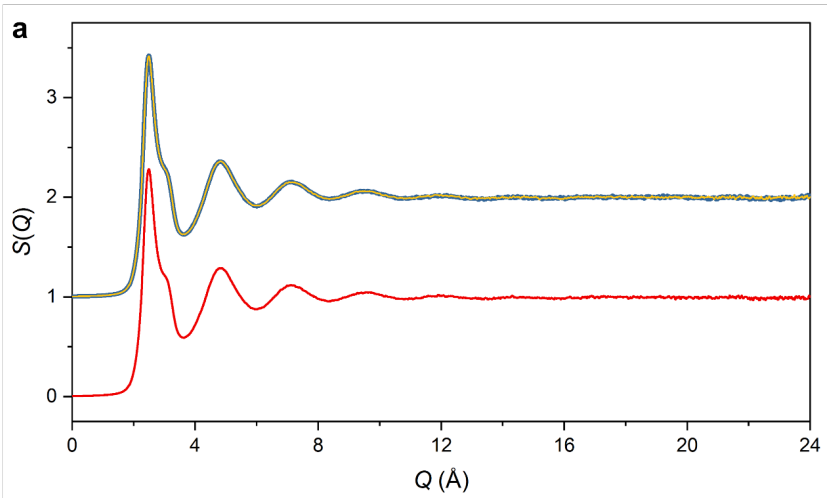

1

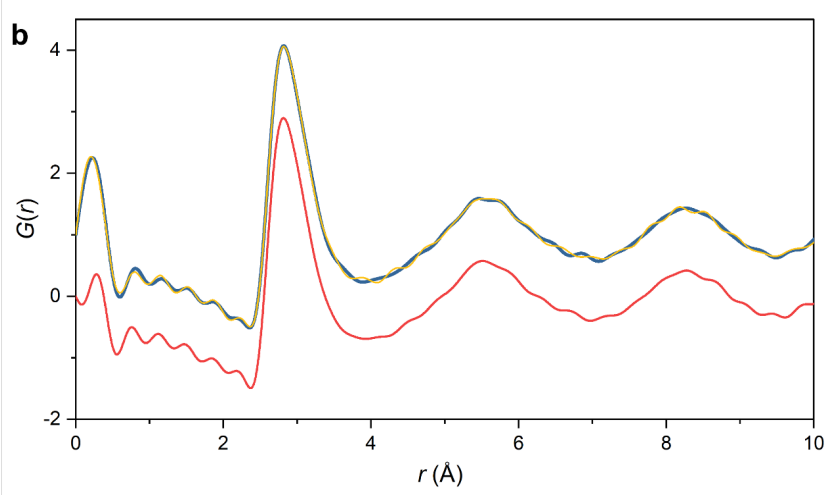

2

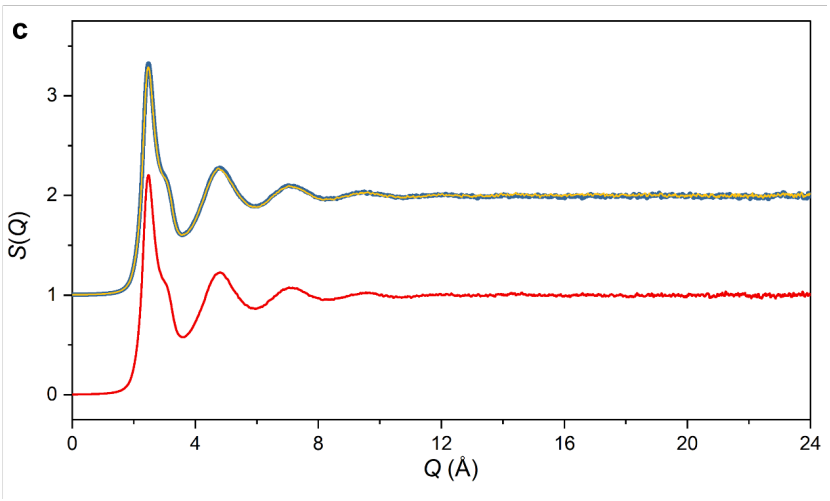

3

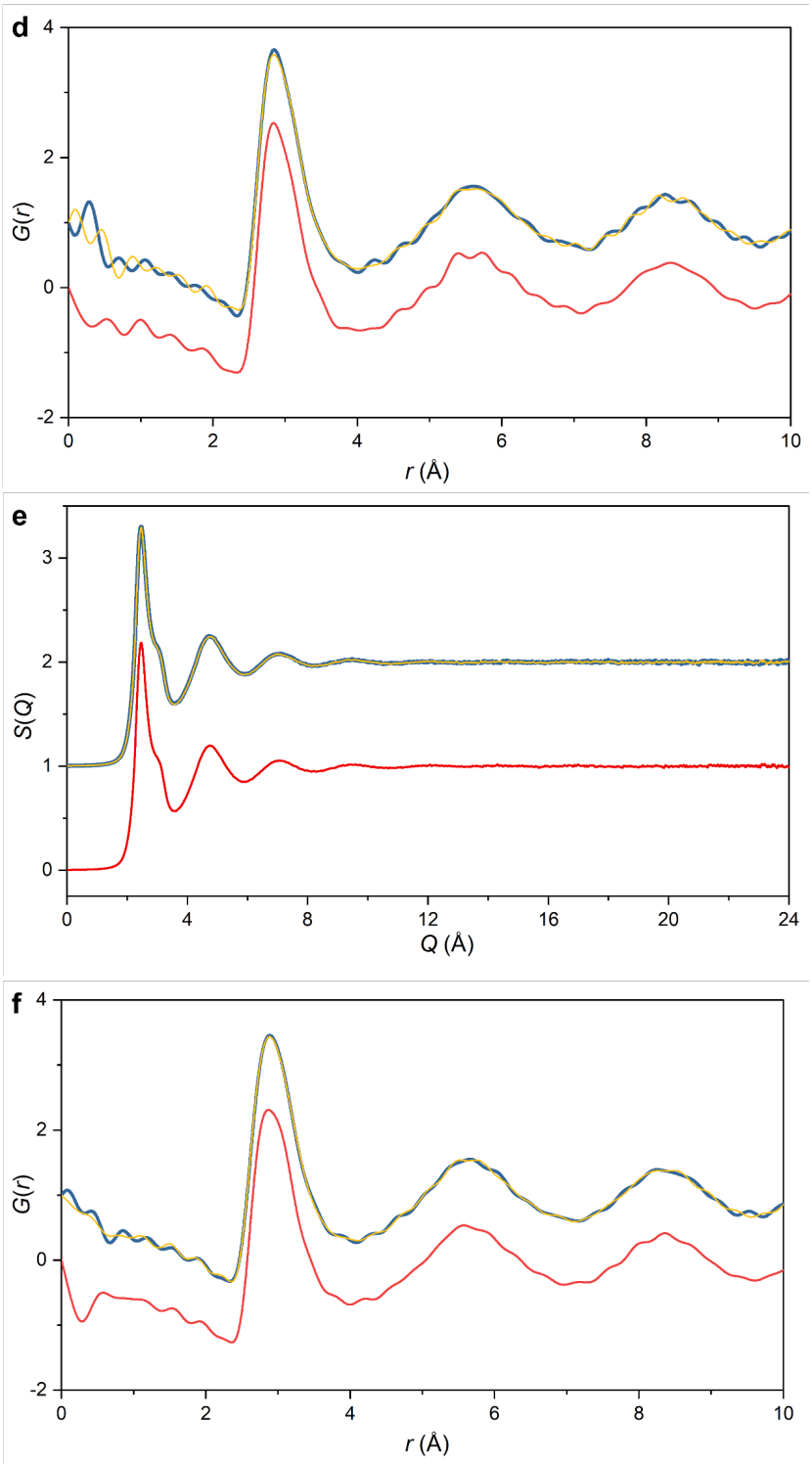

Fig. S2. Structure factors, $S(Q)$ and reduced pair distribution functions, $G(r)$ of liquid metal samples with 0 T (blue curves), 0.2 T SMF (red curves) and SMF removed (yellow curves) **(a-b)** $EGa_{90}In_{10}$; **(c-d)** $EGa_{87}In_{13}$; **(e-f)** $EGa_{85}In_{15}$.

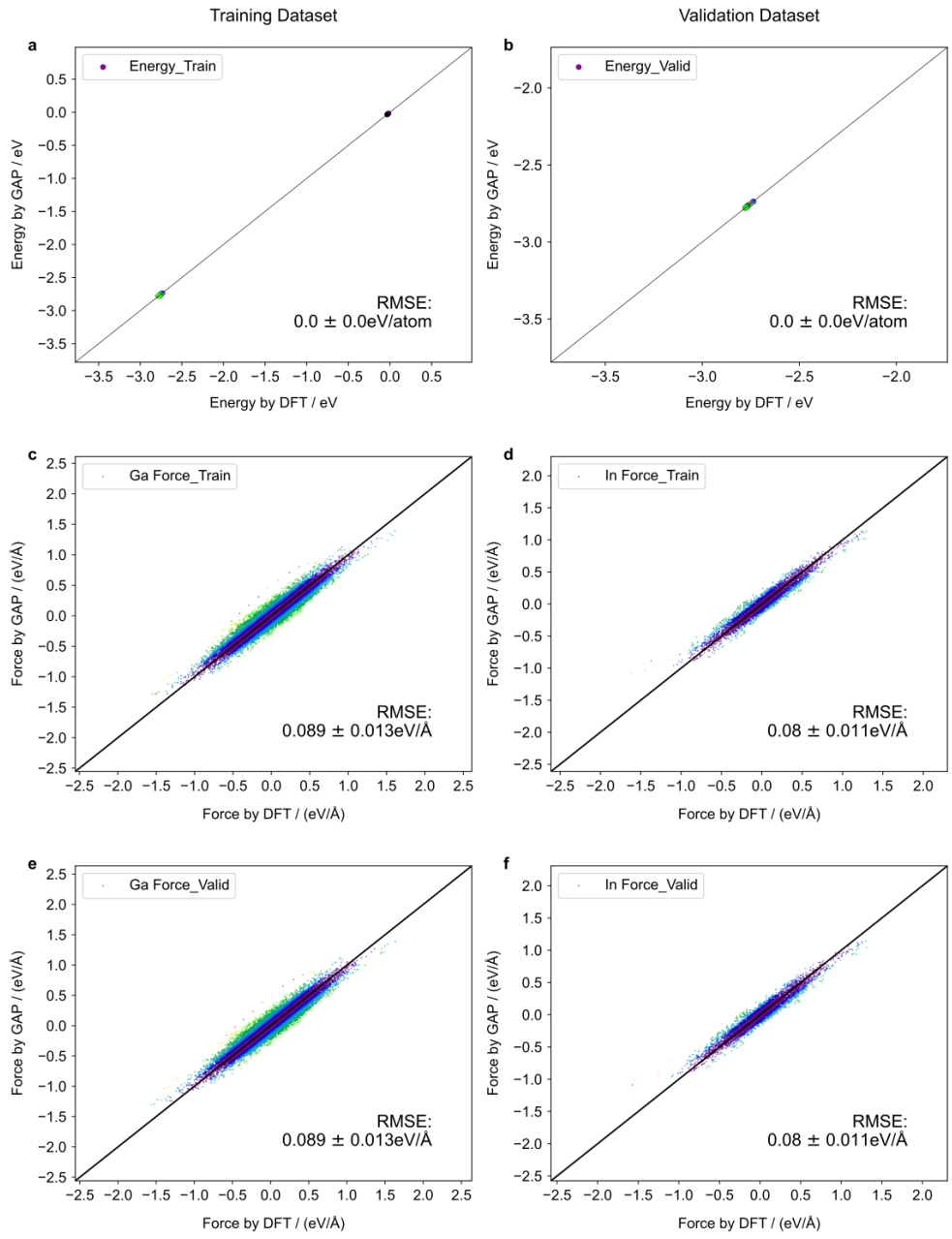

Fig. S3. To validate the Machine Learning Force Field, scattering diagrams are created to compare the predicted energies **(a-b)** and forces of Ga **(c-d)** and In **(e-f)** with the results of DFT computations. Diagrams include both the validation set **(b, d, f)** and training set **(a, c, e)** of structures, with the Relative Mean Square Error (RMSE) marked for each set.

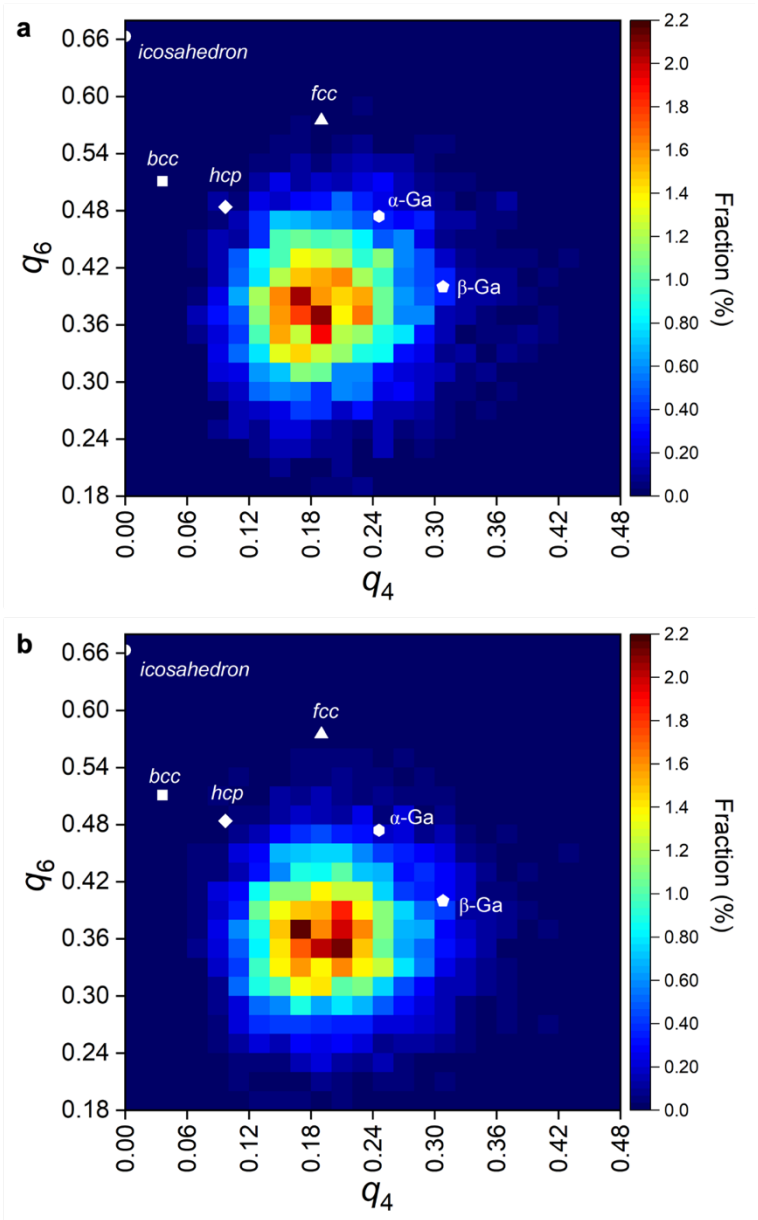

Fig. S4. $q_4 - q_6$ heatmaps for **(a)** 0 T and **(b)** 0.2 T SMF, where the red area represents concentration area of SRO structures. Clearly, the distribution is more concentrated under 0 T, while it becomes more dispersed when applying the 0.2 T field. Additionally, symbols in heatmaps indicate the (q_4, q_6) points of ideal ordered structures, where bcc coordination number (CN) =14 (0.036, 0.511), hcp (0.097, 0.484), fcc (0.190, 0.575), icosahedral (0, 0.663), α-gallium (0.246, 0.474), β-gallium (0.308, 0.400).

Table S1. Structural information derived from total scattering experiments for samples under without SMF (0 T), with 0.2 T SMF and SMF removed conditions.

Parameters \ Samples		$EGa_{90}In_{10}$	$EGa_{87}In_{13}$	$EGa_{85}In_{15}$
$S(Q_1)$	0 T	2.42	2.33	2.30
	0.2 T SMF	2.28	2.20	2.19
	SMF Removed	2.42	2.29	2.30
$S(Q_2)/S(Q_1)$	0 T	0.560	0.550	0.543
	0.2 T SMF	0.565	0.557	0.547
	SMF removed	0.563	0.554	0.542
r_1	0 T	2.82	2.85	2.89
	0.2 T SMF	2.81	2.84	2.87
	SMF removed	2.82	2.84	2.88
$G(r_1)$	0 T	3.07	2.66	2.46
	0.2 T SMF	2.90	2.53	2.31
	SMF removed	3.06	2.58	2.44
CN	0 T	11.08	11.12	11.23
	0.2 T SMF	10.90	10.97	11.02
	SMF removed	11.05	11.07	11.20
ρ_0	0 T	0.0511	0.0481	0.0511
	0.2 T SMF	0.0510	0.0494	0.0510
	SMF removed	0.0513	0.0488	0.0513

Notes: $S(Q_2)/S(Q_1)$ is the ratio of the first two $S(Q)$ peak heights; r_1 is the position of the first peak in $G(r)$; $G(r_1)$ is the height of the first $G(r)$ peak; CN is the nearest-neighbor coordination numbers (see Methods). The average number density of liquid metal samples, ρ_0 is the average atomic number density, derived from the slope of $G(r)$ at low-r area (see Methods).